# The Empirical Dependence of Tornadogenesis on Elevation Roughness: Historical Record Analysis Using Bayes's Law in Arkansas

ZHANXIANG HUA AND DANIEL R. CHAVAS

*Department of Earth, Atmospheric, and Planetary Sciences, Purdue University, West Lafayette, Indiana*

(Manuscript received 22 August 2018, in final form 4 December 2018)

ABSTRACT

Recent research suggests that surface elevation variability may influence tornado activity, though separating this effect from reporting biases is difficult to do in observations. Here we employ Bayes's law to calculate the empirical joint dependence of tornado probability on population density and elevation roughness in the vicinity of Arkansas for the period 1955–2015. This approach is based purely on data, exploits elevation and population information explicitly in the vicinity of each tornado, and enables an explicit test of the dependence of results on elevation roughness length scale. A simple log-link linear regression fit to this empirical distribution yields an 11% decrease in tornado probability per 10-m increase in elevation roughness at fixed population density for large elevation roughness length scales (15–20 km). This effect increases by at least a factor of 2 moving toward smaller length scales down to 1 km. The elevation effect exhibits no time trend, while the population bias effect decreases systematically in time, consistent with the improvement of reporting practices. Results are robust across time periods and the exclusion of EF1 tornadoes and are consistent with recent county-level and gridded analyses. This work highlights the need for a deeper physical understanding of how elevation heterogeneity affects tornadogenesis and also provides the foundation for a general Bayesian tornado probability model that integrates both meteorological and nonmeteorological parameters.

## 1. Introduction

A tornado is a rapidly rotating column of air in contact with the surface and a cumuliform cloud (Agee 2014). The latter is typically associated with a rotating, mesoscale convective storm that forms within a thermodynamic environment characterized by strong low-level wind shear and significant convective available potential energy for low-level air parcels (Thompson et al. 2004; Grams et al. 2012). Much research attention has been devoted to improving the understanding and prediction of tornadoes and their parent storms based on meteorological variables (e.g., Lawson et al. 2018; Allen et al. 2015). Meanwhile, given that a tornado is also in contact with the surface, variations in surface properties, particularly elevation, may also significantly affect tornado formation, structure, and evolution. However, the role of surface heterogeneity in modulating tornado activity remains poorly understood.

Past work has identified numerous complexities in how surface heterogeneity affects tornadoes via a variety of research techniques. Historical case study analysis has demonstrated that tornadoes may form along preferred terrain orientations such as ridges and valleys (Gallimore and Lettau 1970), including within large mountain ranges (Prociv 2012). Topography may enhance tornadogenesis both directly via vortex stretching in downslope flow and indirectly by promoting development of the parent convective cell via enhanced mesoscale low-level wind shear caused by near-surface flow channeling (Homar et al. 2003; LaPenta et al. 2005; Bosart et al. 2006; Schneider 2009; Knupp et al. 2014). Importantly, these case studies highlight that multiple length scales of elevation variability may be important. Laboratory experiments and simulations have demonstrated that surface roughness heterogeneity associated with variations in land cover can directly impact the velocity structure of tornado-like vortices (Lewellen et al. 2008; Natarajan 2011; Lewellen 2014; Bodine et al. 2016) as well as the formation of multiple vortices (Leslie 1977). More recently, idealized atmospheric numerical modeling has demonstrated that variations in orographic geometry can impose significant effects on supercell evolution and potentially on tornado evolution as well (Lewellen 2014).

*Corresponding author*: Daniel R. Chavas, drchavas@gmail.com

DOI: 10.1175/JAMC-D-18-0224.1

While tornado–terrain interactions are clearly complex, past work has also sought generalized relationships between tornadoes and elevation variability by applying statistical methods to historical data. Gallimore and Lettau (1970) found a reduction in tornado activity in Arkansas and Wisconsin in low elevation roughness regions by comparing cross-sectional elevation power spectra in low- and high-tornado regions, and they further identified a critical length scale of elevation roughness of either 1 or 16 km below which this signal emerges. However, the authors acknowledged at the time that potential reporting biases may be significant, an effect that is now widely understood to be large in the historical record (Doswell and Burgess 1988; Doswell 2007; Verbout et al. 2006; Elsner et al. 2013). Karpman et al. (2013) also found a decrease in tornado activity with increasing topographic variability using a multiplicative point-process model that takes as its topographic variability parameter the integrated elevation variance over an approximately 5-km radius, though this study again does not account for population bias. Population bias effects were accounted for by Jagger et al. (2015) and Elsner et al. (2016), who found a similar elevation roughness effect over the Great Plains by modeling tornado activity conditioned on elevation roughness and population density using a negative binomial statistical model fit to tornado, elevation, and population density data binned either at the county level or on a regular grid.

Here we build upon the work of Elsner et al. (2016) by demonstrating a simpler and more general approach using Bayes's law to estimate the joint dependence of tornado activity on elevation variability and population density. We apply this method to historical data in the vicinity of Arkansas. This approach offers three principal benefits: 1) the complete joint dependence is calculated directly from the data, in the absence of statistical modeling assumptions, allowing for direct inspection of the structure of this dependence; 2) the calculation exploits information regarding elevation and population explicitly in the vicinity of each individual historical tornado; and 3) the methodology uses physical length scales relative to individual tornado events, enabling a direct empirical test for the existence of an optimal elevation roughness length scale as well as providing a potential bridge between empirical results and physical modeling. A simple statistical model is then applied a posteriori to quantify the magnitude of these conditional dependencies. Our analysis focuses on Arkansas because the region possesses a wide range of small-scale elevation variability in the absence of major mountain ranges that rise above the boundary layer and thus can substantially disrupt the large-scale atmospheric flow (Manabe and Terpstra 1974). Moreover, focusing on a limited area minimizes variability in environmental thermodynamic heterogeneity on climatological time scales, thereby credibly separating nonmeteorological effects (population and elevation) from meteorological effects associated with large-scale atmospheric variability. Overall, then, Arkansas provides an ideal region to search for a statistical signature of elevation roughness on tornado activity. We note that such a physical effect, should it exist in nature and be isolated empirically, ought to be generalizable to any region that possesses variability in terrain elevation. Thus, our results need not be specific to Arkansas, and indeed we compare our results to those of prior analyses in other regions. Finally, we examine the robustness of this joint dependence to varying time period, EF rating, and terrain length scale. The latter tests for the potential existence of a preferred physical length scale of the effect of elevation variability on tornadogenesis.

The paper is organized as follows. Section 2 describes the datasets and Bayes's law theory and methodology. Section 3 presents the results for a step-by-step demonstration application followed by more general results testing for robustness. Section 4 provides a summary and discussion of the significance of this work as well as avenues of future research.

## 2. Methodology

### a. Data

We combine historical tornadogenesis data within the domain bounded by 90.2408°–95.2366°W longitude and 32.8134°–37.1342°N latitude, which encompasses the state of Arkansas, with historical population density and elevation data within a slightly larger domain bounded by 90°–96°W longitude and 32°–38°N latitude.

Tornadogenesis latitude, longitude, year, and intensity (EF) rating data are taken from the NOAA Storm Prediction Center database for the period 1955–2015 (https://www.spc.noaa.gov/wcm/#data, accessed 18 March 2016) (Fig. 1a). This dataset has a range of known and unknown data reporting and quality biases (Doswell and Burgess 1988; Doswell 2007); nonetheless, it is by far the most comprehensive database available whose relatively large sample size lends itself well to empirical analysis. EF0 events have especially large empirical, societal, and physical reporting biases (Verbout et al. 2006; Agee and Childs 2014; Tippett et al. 2015) and are thus discarded. The resulting dataset contains 1991 EF1–5 tornadoes and 855 EF2–5 tornadoes. Population density data at 30-arc-s resolution (≈0.76 km at 35° latitude) are obtained from version 4 of the Columbia University Gridded Population of the World dataset (http://sedac.ciesin.columbia.edu/data/set/gpw-v4-population-density) for the year 2015, and time-varying population density data at

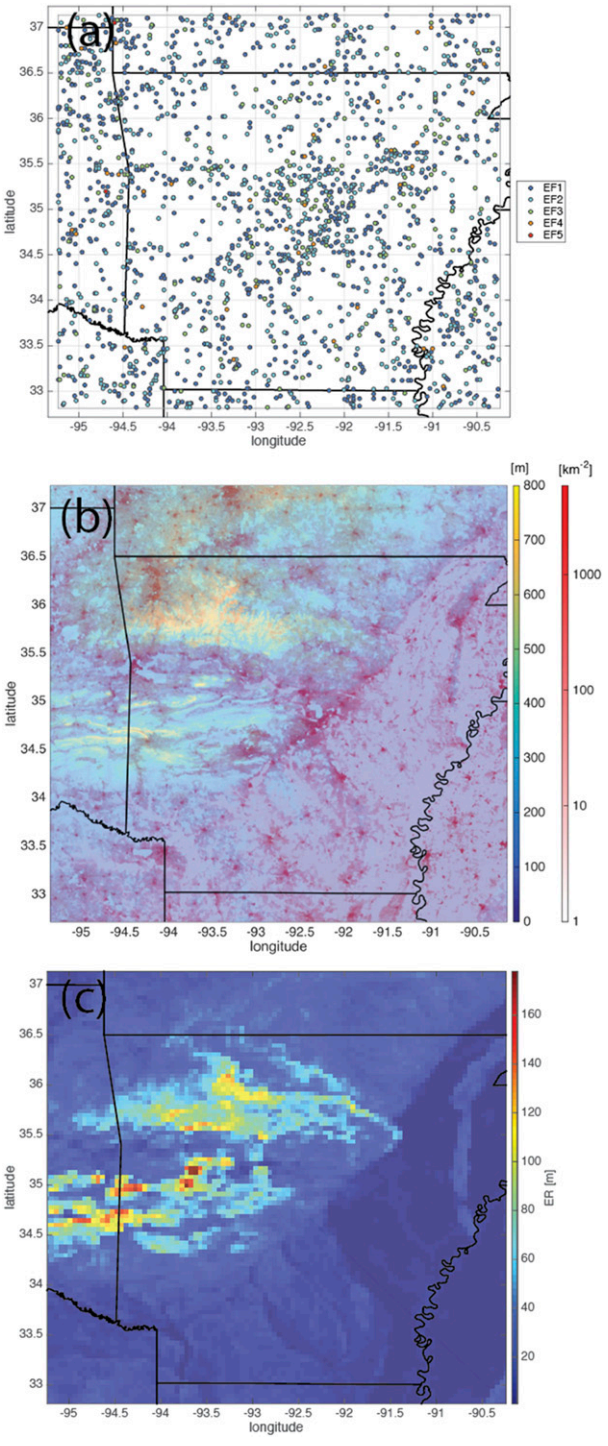


FIG. 1. Spatial distributions of (a) tornadogenesis points (1955–2015); (b) surface elevation (color) and 2015 raw population density (red shading; log scale); and (c) elevation roughness ($ER_b$) for $L_{ER}$ = 10 km, calculated on uniform 100 × 100 grid as described in section 2. Gray box in (a) demarcates tornado domain boundaries.

30-arc-s resolution are taken from Global Population Density Grid Time Series Estimates, version 1 (1970–2000) (http://sedac.ciesin.columbia.edu/data/set/popdynamics-global-pop-density-time-series-estimates) for years 1970, 1980, 1990, and 2000. Terrain elevation raster data at 7.5-arc-s resolution (≈0.19 km at 35° latitude) are obtained from the Global Multiresolution Terrain Elevation Data 2010 (GMTED2010) (https://www.usgs.gov/land-resources/eros/coastal-changes-and-impacts/gmted2010, downloaded from https://earthexplorer.usgs.gov/). Terrain and population density datasets are cropped to the analysis region (Fig. 1b) using the clipper tool in QGIS, version 2.18 (QGIS 2015). All subsequent statistical analyses are performed using MATLAB R2015a. All geographic area and distance calculations assume a sphere with radius $r$ = 6371.22 km.

### b. Variable definitions

Annual tornado probability per unit area (hereafter "tornado probability") $P(T)$ [No. yr$^{-1}$ (100 km$^2$)$^{-1}$], is defined as

$$P(T) = \frac{\sum_{i,y} T_{yi}}{YA} \times 100, \qquad (1)$$

where $T_{yi}$ corresponds to tornado $i$ in year $y$, $Y$ is the number of years (e.g., 61 for 1955–2015), $A$ is the domain area (e.g., $A$ = 218 660 km$^2$ for the full domain), and the factor 100 normalizes the base probability (No. yr$^{-1}$ km$^{-2}$) to a constant reference area of 100 km$^2$. This quantity may be equivalently thought of as a space–time tornado density.

Population density, (lpop; No. km$^{-2}$, log2-transformed), is calculated via simple bilinear interpolation of the raw data to a point of interest and then taking the base-2 logarithm. The logarithm is applied because this quantity varies over many orders of magnitude. Moreover, population biases may be expected to scale multiplicatively, for example, an increase from 1 to 10 people per unit area is likely more similar to an increase from 1000 to 10 000 than from 1000 to 1009.

Elevation roughness (ER; m) is defined as the standard deviation of all elevation values at radii $r \leq R$; this quantity is the simplest statistical measure of spatial variability. The associated length scale of variability is defined as $L_{ER} = 2R$ (i.e., circle diameter), and we present results over the range $L_{ER} \in [1, 20]$ . Length scales smaller than 1 km approach the intrinsic resolution of the terrain data and thus yield sample sizes too small to calculate a credible standard deviation. We choose $L_{ER}$ = 10 km for demonstration in the analyses below before presenting final results across the full range of values; the spatial distribution of this quantity is displayed in Fig. 1c. Importantly, elevation standard deviation is a physical variable

with meaningful units that we seek to preserve in our analysis.

Integral to the Bayes's law approach described in the next subsection, population density and elevation roughness are calculated at locations spread uniformly within the domain as well as at all tornadogenesis locations. This yields datasets for both background population density ($\text{lpop}_b$) and elevation roughness ($\text{ER}_b$) as well as tornado-centered population density ($\text{lpop}_T$) and elevation roughness ($\text{ER}_T$).

### c. *Conditional probability analysis: Bayes's law*

We seek to quantify the joint dependence of tornado probability on elevation roughness and population density, that is, $P(T|\text{ER, lpop})$. From the definition of conditional probability, we may write

$$P(T, \text{ER}, \text{lpop}) = P(T|\text{ER}, \text{lpop})P(\text{ER}, \text{lpop}). \quad (2)$$

This probability may be equivalently written as

$$\begin{aligned} P(T, \text{ER}, \text{lpop}) &= P(\text{ER, lpop}|T)P(T) \\ &= P(\text{ER}_T, \text{lpop}_T)P(T), \end{aligned} \quad (3)$$

where $\text{ER}_T$ and $\text{lpop}_T$ denote the elevation roughness and population density conditioned on a tornado, that is, in the vicinity of a tornado. Equating the right-hand sides of Eqs. (2) and (3) and rearranging yields an equation for the conditional probability $P(T|\text{ER, lpop})$ given by

$$P(T|\text{ER}, \text{lpop}) = \left[\frac{P(\text{ER}_T, \text{lpop}_T)}{P(\text{ER}_b, \text{lpop}_b)}\right] P(T), \quad (4)$$

where $\text{ER}_b$ and $\text{lpop}_b$ denote the background elevation roughness and population density within the domain; this notation is used on the rhs of Eq. (4) to clearly distinguish these quantities from their tornado-conditioned counterparts. Equation (4) is simply Bayes's law applied to our conditional tornado probability, in which a prior terrain- and population-independent tornado probability $P(T)$ is updated with information about elevation roughness and population density to yield a posterior (conditional) tornado probability $P(T|\text{ER, lpop})$. The Bayesian update factor is defined in Eq. (4) as the ratio of the joint probability of elevation roughness and population density in the vicinity of a tornado to their joint probability anywhere within the domain (i.e., independent of tornado). In words, Eq. (4) states that the tornado probability increases relative to some average value $P(T)$ if $P(\text{ER}_T, \text{lpop}_T) > P(\text{ER}_b, \text{lpop}_b)$, that is, if the probability of finding a certain combination of $(\text{ER}_0, \text{lpop}_0)$ is higher in the vicinity of a tornado than in general in the entire domain. In such a case, the update factor will be greater than one, and thus $P(T|\text{ER, lpop}) > P(T)$.

All three probabilities on the right-hand side of Eq. (4) can be calculated directly from historical data. The terrain- and population-independent tornado probability $P(T)$ is calculated by applying Eq. (1) for all tornadoes in the full domain, that is, the domainwide mean tornado probability. For terrain- or population-dependent probabilities, we discretize ER and lpop into fixed-width bins of $\Delta\text{ER} = 10\,\text{m}$ and $\Delta\text{lpop} = 0.5$ beginning at zero for both quantities, which yields a reasonable number of bins in each dimension. We estimate the joint distribution $P(\text{ER}_b, \text{lpop}_b)$ by calculating (ER, lpop) on a uniformly spaced $100 \times 100$ latitude–longitude grid bounded by our tornadogenesis domain, yielding a background sample size of 10 000. This grid is used in lieu of direct calculation using the raw population density dataset grid ($720 \times 720$) to reduce computational costs while still maintaining a sufficiently large sample size to properly define the distribution. Similarly, we estimate the joint distribution $P(\text{ER}_T, \text{lpop}_T)$ by calculating (ER, lpop) at all tornadogenesis points in our dataset.

Marginal probabilities are calculated for the general case as

$$P(x_b) = \frac{n\{x_b \in [x^j, x^{j+1})\}}{N}, \quad (5)$$

and for the tornado-centered case as

$$P(x_T) = \frac{n\{x_T \in [x^j, x^{j+1})\}}{N}, \quad (6)$$

where $x$ represents ER or lpop, $n\{x \in [x^j, x^{j+1})\}$ is the number of points whose value falls within the $j$th interval bounded by $x^j$ and $x^{j+1}$, and $N$ is the full sample size of points (10 000 for background; total number of tornadoes for tornado centered). Similarly, joint probabilities are calculated for the general case as

$$P(x_{1,b}, x_{2,b}) = \frac{n\{x_{1,b} \in [x_1^j, x_1^{j+1}), x_{2,b} \in [x_2^j, x_2^{j+1})\}}{N}, \quad (7)$$

and for the tornado-centered case as

$$P(x_{1,T}, x_{2,T}) = \frac{n\{x_{1,T} \in [x_1^j, x_1^{j+1}), x_{2,T} \in [x_2^j, x_2^{j+1})\}}{N}, \quad (8)$$

where $x_1$ and $x_2$ represent ER and lpop.

Combining these probabilities according to Eq. (4) yields an empirical estimate of $P(T|\text{ER, lpop})$. However, we note that the essence of this analysis lies in an understanding of the joint dependence of the Bayesian update factor; this factor is simply mapped into probability

space via multiplication by a constant mean tornado probability $P(T)$ that is specific to the given geographic domain and time period.

### d. Statistical modeling

Finally, we quantify the magnitude of the dependence of tornado probability on both elevation roughness and population density by fitting a generalized linear model (GLM; Nelder and Baker 2004) with a bivariate log-link response function (also known as Poisson regression) to our calculated conditional probabilities, that is,

$$\ln[P(T|\mathrm{ER},\mathrm{lpop})] = \beta_0 + \beta_{\mathrm{ER}}\mathrm{ER} + \beta_{\mathrm{lpop}}\mathrm{lpop} + \varepsilon, \quad (9)$$

where $\beta_{\mathrm{ER}}$ and $\beta_{\mathrm{lpop}}$ are the regression coefficients to elevation roughness and population density, respectively; $\beta_0$ is a constant; and $\varepsilon$ is the model residual error. Thus, this model yields $P(T|\mathrm{ER}, \mathrm{lpop}) = ce^{\beta_{\mathrm{ER}}\mathrm{ER}+\beta_{\mathrm{lpop}}\mathrm{lpop}}$, where $c$ is a constant. The log-link response function is chosen because tornado probability is a nonnegative quantity and thus standard linear regression is inappropriate. We emphasize that the form of the statistical model is not fundamental to the result; here we choose as simple a model as possible whose outcome is easy to interpret. The best fit is determined via linear least squares fit of $\ln[P(T|\mathrm{ER}, \mathrm{lpop})]$ to the data using MATLAB function glmfit. In fitting the model, we exclude $(\mathrm{ER}_b, \mathrm{lpop}_b)$ bins with bin sample size less than five in the background joint distribution; for very small bin sample sizes, the Bayesian update factor is very sensitive to a small changes in tornado count (e.g., from 0 to 1). This choice ensures that the results of the statistical model fit apply to a reasonably common range of values of $(\mathrm{ER}_b, \mathrm{lpop}_b)$.

For each analysis, we perform a 1000-member bootstrap ensemble in which we redo the full analysis using 1000 resamples of the tornado dataset and its associated tornado-centered covariate values $(\mathrm{ER}_T, \mathrm{lpop}_T)$. We then define the best estimate of each coefficient as the median of their respective bootstrapped distributions, and we define the 5%–95% confidence band for our model coefficients as the 5th and 95th percentiles of the distribution. Bootstrapping is both flexible and robust, as it makes no assumptions about the nature of the input or output distributions and permits asymmetric confidence bands (Mooney et al. 1993).

## 3. Results

### a. Demonstration application

We begin with a step-by-step demonstration application for the case of all EF1+ tornadoes for the full period 1955–2015 with calculation length scale $L_{\mathrm{ER}} = 10$ km.

#### 1) Average tornado probability: $P(T)$

For period length $Y = 61$ years, 1991 EF1+ tornadoes, and domain area $A = 218\,660\,\mathrm{km}^2$, Eq. (1) yields $P(T) = 0.0149\,\mathrm{yr}^{-1}\,(100\,\mathrm{km}^2)^{-1}$. This translates to approximately 1.49 tornadoes per 1° × 1° latitude–longitude box annually within this latitude band.

#### 2) Marginal probability distributions: $P(\mathrm{ER}_b)$, $P(\mathrm{lpop}_b)$, $P(\mathrm{ER}_T)$, $P(\mathrm{lpop}_T)$

Prior to calculating the update factor probabilities of Eq. (4), it is instructive to first quantify marginal probability distributions for elevation roughness and population density and compare the general case to that centered on a tornado. Note that these probabilities are intrinsic to the joint probabilities of Eq. (4) via the definition of conditional probability, for example, $P(\mathrm{ER}_b, \mathrm{lpop}_b) = P(\mathrm{ER}|\mathrm{lpop}_b)P(\mathrm{lpop}_b)$.

All four marginal probability distributions are shown in Fig. 2. The distribution of $\mathrm{ER}_T$ is shifted toward lower values relative to that of $\mathrm{ER}_b$, indicating a preference for tornadoes to form in the presence of smaller elevation roughness relative to the background distribution. Meanwhile, the distribution of $\mathrm{lpop}_T$ is shifted toward higher values relative to that of $\mathrm{lpop}_b$, indicating the population bias associated with increased likelihood that a tornado will be observed or its intensity properly quantified in regions with higher population density relative to the background distribution. While this offers initial intuitive insight, the two quantities are correlated and thus separating the independent effects of each necessitates analysis of their joint probability.

#### 3) Joint probability distributions: $P(\mathrm{ER}_b, \mathrm{lpop}_b)$ and $P(\mathrm{ER}_T, \mathrm{lpop}_T)$

The distributions of joint probabilities $P(\mathrm{ER}_b, \mathrm{lpop}_b)$ and $P(\mathrm{ER}_T, \mathrm{lpop}_T)$ are displayed in Fig. 3. The joint distribution of $P(\mathrm{ER}_b, \mathrm{lpop}_b)$ (Fig. 3a) indicates that land most frequently possesses a combination of relatively low elevation roughness and moderate population density, as might be expected based on the marginal distributions of Fig. 2. Importantly, though, a wide range of $(\mathrm{ER}_b, \mathrm{lpop}_b)$ values exist in our domain, including low $\mathrm{ER}_b$ at high $\mathrm{lpop}_b$ and vice versa, thereby offering hope of statistically separating the terrain signal from that associated with population density bias. Meanwhile, the distribution of $P(\mathrm{ER}_T, \mathrm{lpop}_T)$ appears to shift toward lower $\mathrm{ER}_b$ and higher $\mathrm{lpop}_b$ values (Fig. 3b); the significance of this shift is directly manifest in the update factor distribution analyzed next.

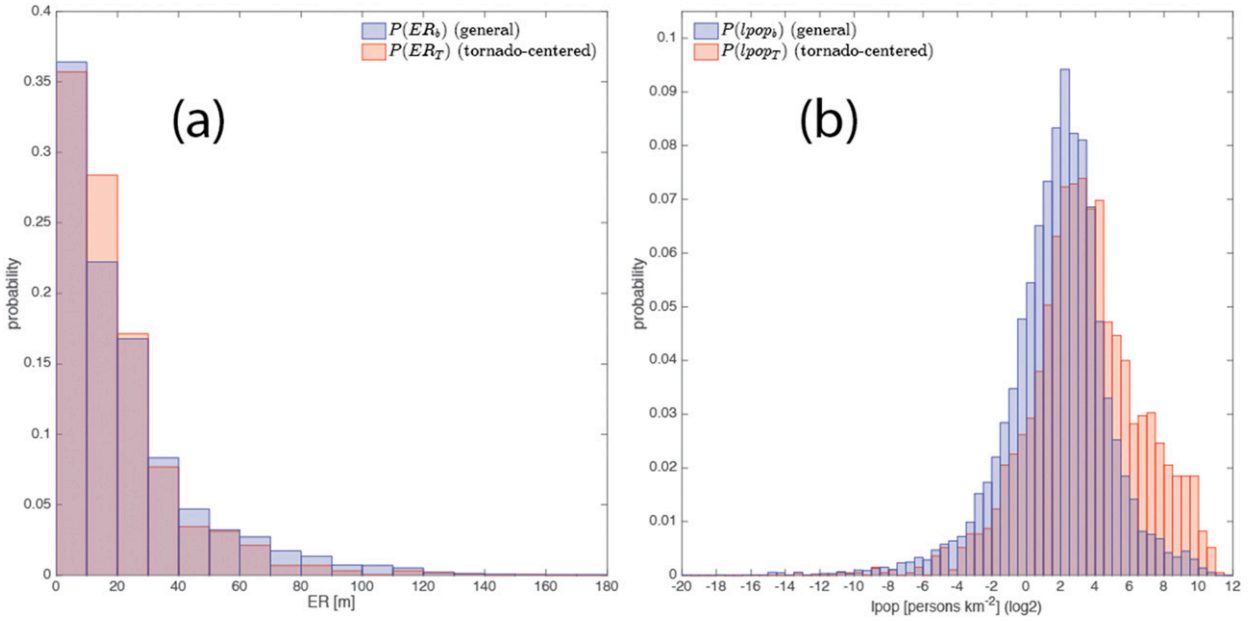


FIG. 2. Probability distributions of (a) $\mathrm{ER}_b$ (blue) and $\mathrm{ER}_T$ (red) for $L_{\mathrm{ER}} = 10$ km and of (b) $\mathrm{lpop}_b$ (blue) and $\mathrm{lpop}_T$ (red).

#### 4) FINAL CONDITIONAL PROBABILITY: $P(T|\mathrm{ER}, \mathrm{lpop})$

Distributions of the Bayesian update factor, defined as the ratio of the joint probabilities presented in Fig. 3, and the final conditional probability $P(T|\mathrm{ER}, \mathrm{lpop})$ calculated by Eq. (4) are both shown in Fig. 4. Recall that the final conditional probability distribution is given simply by the product of the update factor and the average tornado probability in the domain. An update factor value larger than 1 indicates $P(T|\mathrm{ER}, \mathrm{lpop}) > P(T)$, and a value smaller than 1 indicates $P(T|\mathrm{ER}, \mathrm{lpop}) < P(T)$.

A broad reduction in tornado probability is evident moving toward both lower population density and higher elevation roughness. This may be interpreted alternatively as a decrease in tornado probability with increasing

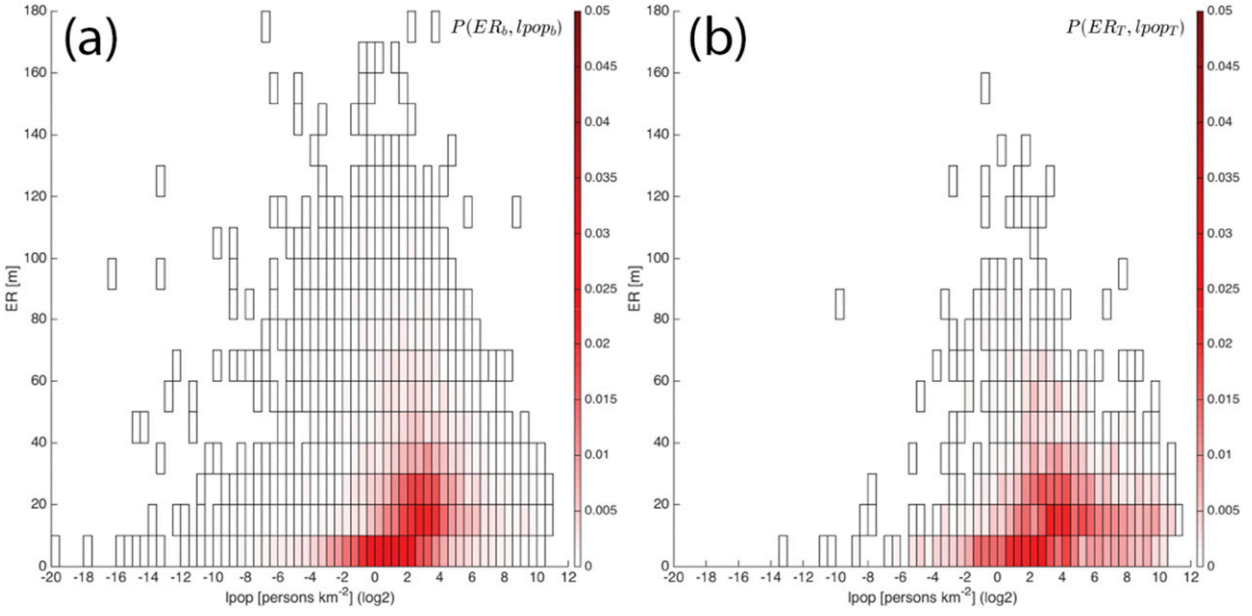


FIG. 3. Joint probability distributions (a) $P(\mathrm{ER}_b, \mathrm{lpop}_b)$, and (b) $P(\mathrm{ER}_T, \mathrm{lpop}_T)$, corresponding to the denominator and numerator, respectively, of the Bayesian update factor in Eq. (4) for $L_{\mathrm{ER}} = 10$ km. Boxes indicate bins containing at least one valid data point.

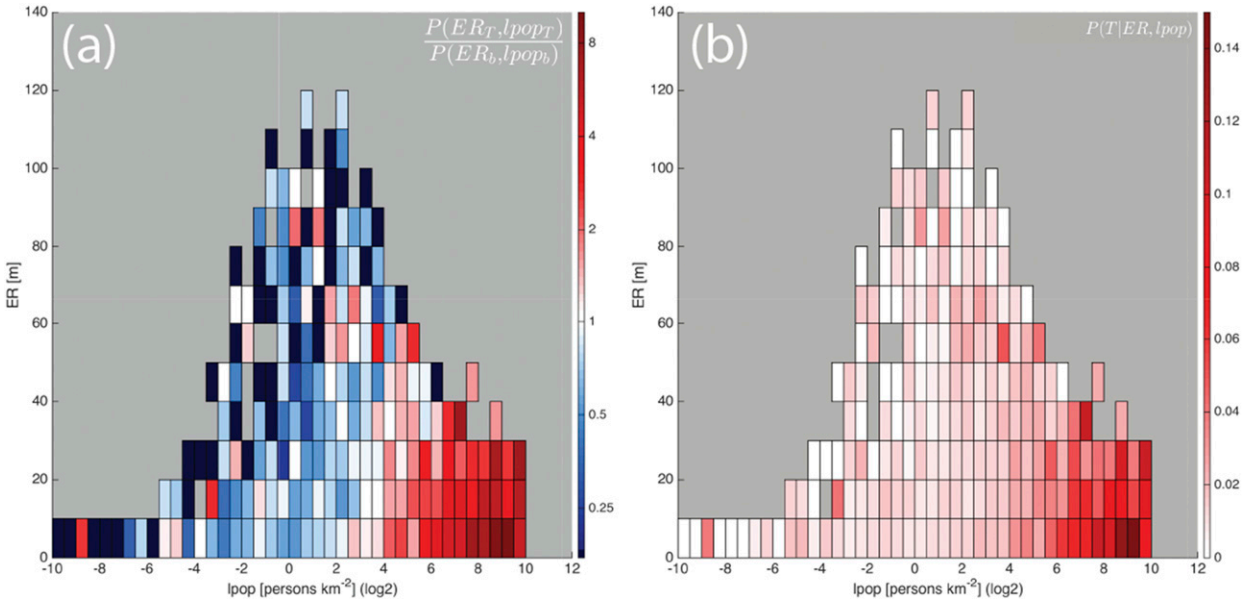


FIG. 4. Distributions of (a) Bayesian update factor and (b) $P(T|\mathrm{ER}, \mathrm{lpop})$, from Eq. (4) for $L_{\mathrm{ER}} = 10$ km. Bins with sample size less than 5 in $P(\mathrm{ER}_b, \mathrm{lpop}_b)$ are masked out (gray). Zero values in (a) are displayed in darkest blue. The domain-mean tornado probability is $P(T) = 0.0149\,\mathrm{yr}^{-1}\,(100\,\mathrm{km}^2)^{-1}$.

elevation roughness conditioned on (i.e., controlling for) population density. The effect appears consistent over the full range of population density, though it is most readily visible at intermediate population density where elevation roughness varies significantly within a given population density bin. We emphasize that these results arise purely from data; no statistical models have yet been applied. Fitting the log-link GLM model given by Eq. (9) to the data shown in Fig. 4 yields best-fit coefficient values of $\beta_{\mathrm{ER}} = -0.013\,\mathrm{m}^{-1}$ {5%–95% confidence interval (CI) of $[-0.017, -0.010]$} and $\beta_{\mathrm{lpop}} = +0.19$ (5%–95% CI of $[+0.17, +0.21]$).

#### 5) INTERPRETATION

Finally, we seek a basic quantitative interpretation of our elevation roughness coefficient $\beta_{\mathrm{ER}}$. Taking the partial derivative of Eq. (9) with respect to ER yields

$$\beta_{\mathrm{ER}} = \frac{\partial\{\ln[P(T|\mathrm{ER}, \mathrm{lpop})]\}}{\partial(\mathrm{ER})} = \frac{1}{P(T|\mathrm{ER}, \mathrm{lpop})} \frac{\partial[P(T|\mathrm{ER}, \mathrm{lpop})]}{\partial(\mathrm{ER})}, \qquad (10)$$

where $\beta_{\mathrm{ER}}$ is the fractional sensitivity of $P(T|\mathrm{ER}, \mathrm{lpop})$ to varying ER, and $100\beta_{\mathrm{ER}}$ is the percentage rate of change (% $\mathrm{m}^{-1}$) at fixed population density. Thus, $\beta_{\mathrm{ER}} = -0.013\,\mathrm{m}^{-1}$ translates to a 13% decrease in tornado probability for every 10 m increase in elevation roughness.

Similarly, we may quantitatively interpret our population density coefficient $\beta_{\mathrm{lpop}}$ as

$$\beta_{\mathrm{lpop}} = \frac{\partial\{\ln[P(T|\mathrm{ER}, \mathrm{lpop})]\}}{\partial(\mathrm{lpop})} = \frac{\partial\{\ln[P(T|\mathrm{ER}, \mathrm{lpop})]\}}{\partial[\ln(\mathrm{pop})]} \times \ln(2), \qquad (11)$$

where pop is the raw population density and we have transformed the base-2 logarithm to a natural logarithm using the change of base equation, $\log_2(x) = \ln(x)/\ln(2)$. The term $\beta_{\mathrm{lpop}}$ is the percentage rate of change of $P(T|\mathrm{ER}, \mathrm{lpop})$ per percentage change in population density at fixed elevation roughness. Thus, $\beta_{\mathrm{lpop}} = +0.19$ translates to a 1.9% increase in tornado probability for every 10% increase in raw population density. This translates to a 19% increase per doubling of population density, a result that is also evident by retaining the base-2 logarithm in the denominator of Eq. (11), which represents a percentage change per doubling of the raw population density.

### b. *General analysis*

We now examine the sensitivity of our coefficients to calculate length scale, time period, and the exclusion of EF1 tornadoes. Figure 5 displays $\beta_{\mathrm{ER}}$ (Fig. 5a) and $\beta_{\mathrm{lpop}}$ (Fig. 5b) calculated for $L_{\mathrm{ER}} \in [1, 20]$ km using tornado data for the full period 1955–2015, as well as for successive 21-yr overlapping periods 1955–75,

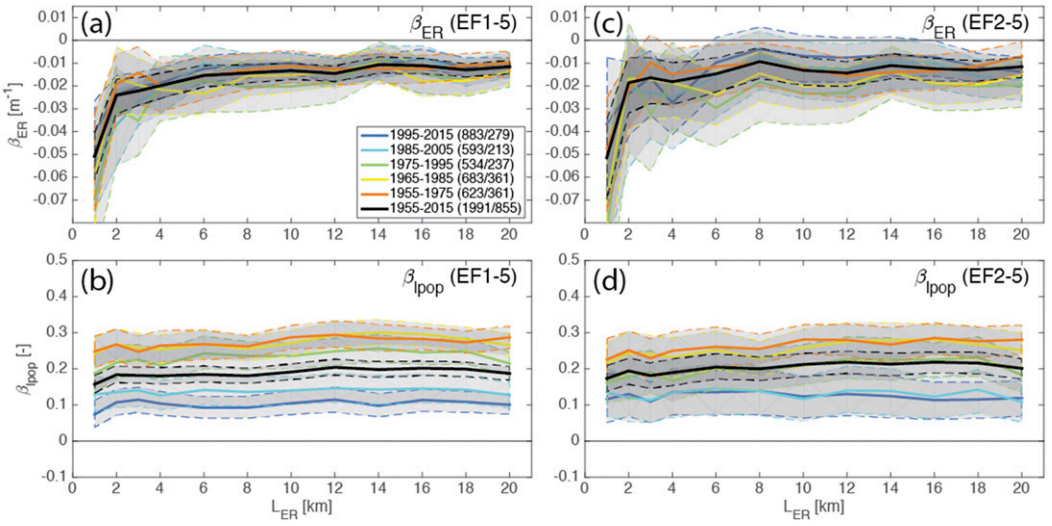


FIG. 5. Coefficients of the log-linked linear model fit to the empirical estimate of $P(T|\text{ER, lpop})$ as a function of calculation length scale $L_{ER}$: (a) elevation roughness coefficient $\beta_{ER}$ and (b) population density coefficient $\beta_{lpop}$. (c),(d) As in (a) and (b), respectively, but for EF2–5 tornadoes. Result are shown for full 1955–2015 period (black) and successive 21-yr periods (color), with 5%–95% confidence intervals (shaded and dashed) calculated from 1000-member bootstrap ensembles. Number of EF1 and EF2 tornadoes in each period also shown in the legend as (EF1/EF2).

1965–85, 1975–95, 1985–2005, and 1995–2015. Identical analyses using only EF2–5 tornado data are also provided (Figs. 5c,d).

First, for the full-period (1955–2015) analysis, the best-fit values and 5%–95% confidence interval are consistently negative for $\beta_{ER}$ and positive for $\beta_{lpop}$, indicating that the qualitative finding of our demonstration example is robust for varying $L_{ER}$. More specifically, $|\beta_{ER}|$ remains nearly constant at approximately 0.011 for $L_{ER} \geq 14$ km and increases with decreasing $L_{ER}$ at first slowly for $L_{ER} \in [6,\ 14]$ km and then more rapidly for $L_{ER} < 6$ km, reaching $\beta_{ER} = -0.024\,\text{m}^{-1}$ for $L_{ER} = 2$ km followed by a particularly strong increase to $\beta_{ER} = -0.051\,\text{m}^{-1}$ for $L_{ER} = 1$ km. Meanwhile, $\beta_{lpop}$ remains nearly constant across all values of $L_{ER}$.

Second, results are robust to the chosen time period within the historical record. Interestingly, there is no systematic time trend in $\beta_{ER}$, whereas there is a clear systematic decrease in $\beta_{lpop}$ moving closer to present. The decrease in $\beta_{lpop}$ is indicative of a decreasing population bias with time as reporting practices improve, including the introduction of radar in the early 1990s and dramatic growth in storm chasing; this result matches that of Elsner et al. (2013). Meanwhile, the lack of time trend in $\beta_{ER}$ is desirable given that the elevation roughness effect is physical and elevation is nearly fixed during the period of interest, as was found in Elsner et al. (2016). Taken together, these results lend further confidence in the credibility of our analysis to separate the elevation roughness effect from a time-varying population bias effect.

Third, all of the above findings appear to be robust to the exclusion of EF1 tornadoes. Best-fit values of both coefficients are quantitatively similar to the original case; confidence intervals are now wider because of the significantly reduced tornado sample size.

Finally, the above analysis uses a static 2015 population density dataset. Thus, we further test the extent to which accounting for changes in population density with time affect these results. We perform the prior analysis for successive 21-yr overlapping periods 1960–80, 1970–90, 1980–2000, and 1990–2010, each centered on decennial population data for 1970–2000. Figure 6 displays the results, which are quantitatively similar to that shown in Fig. 5. This result indicates that these conclusions are not very sensitive to the details of changes in population density with time. This is perhaps a reflection of the fact that we analyze the logarithm of population density, which requires exponential changes in its spatial distribution to induce significant variations.

Overall, these results indicate that the negative effect of elevation roughness on tornadogenesis appears to be strongest at small length scales, consistent with the work of Gallimore and Lettau (1970). The resolution of our terrain data limits our capacity to confidently test even smaller length scales below 1 km. Moreover, the asymptote for large $L_{ER}$ to an 11% decrease in tornado probability for every 10-m increase in elevation roughness is comparable to that found in previous studies in the Great Plains. Specifically, Jagger et al. (2015) found an 18% decrease per 10 m for EF1+ tornadoes over the

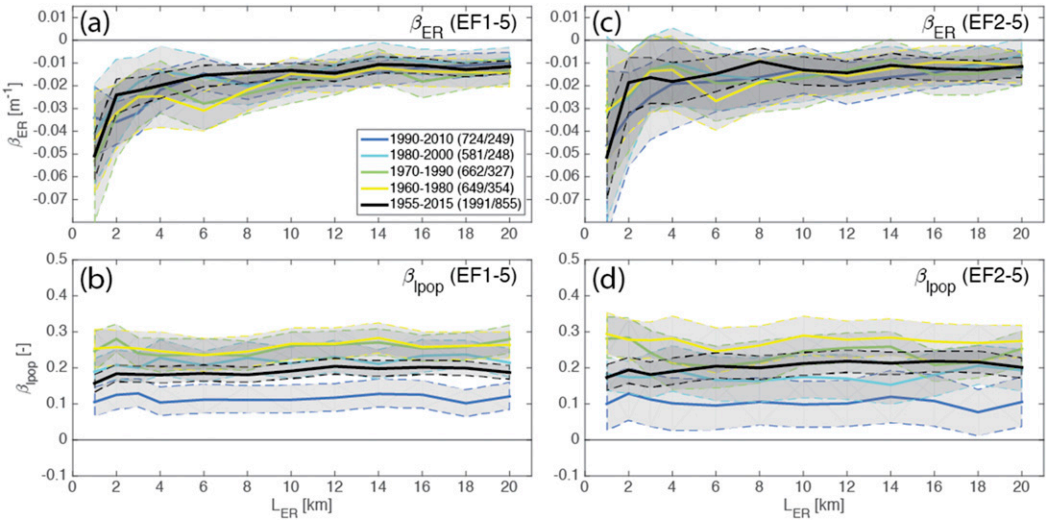


FIG. 6. As in Fig. 5, but using population density data for the midpoint year of successive 21-yr periods (legend).

period 1970–2013 using county-level data, which implicitly averages data over the relatively large length scales associated with county boundaries. Elsner et al. (2016) found a 26% decrease per 10 m for EF1+ tornadoes over the period 1955–2014 using gridded data with horizontal resolution of approximately 23 km; with EF0 events included, this sensitivity decreased slowly from 23% at 23-km resolution to 17% at 6-km resolution (cf. their Table 1). Meanwhile, the population bias effect in each study was 13% and 12% (EF0+) per doubling, respectively. Thus, our results are qualitatively similar though yield a somewhat smaller elevation roughness effect and larger population bias, each by approximately a factor of 2. Further discussion is provided below.

## 4. Discussion and conclusions

This work combines historical tornado, population density, and digital elevation model datasets to quantify the independent effects of varying elevation roughness and population density on the probability of tornadogenesis. Our analysis employs Bayes's law to calculate the probability of tornadogenesis conditioned jointly on elevation roughness (elevation standard deviation) and population density (log2-transformed). This approach provides the most general empirical estimation of this joint conditional probability in the absence of statistical modeling assumptions, enabling direct inspection of the complete structure of the joint dependence. Moreover, it makes explicit use of elevation roughness and population information in the vicinity of individual tornado events. The latter is additionally important for testing the length-scale dependence of elevation roughness in the immediate vicinity of potential tornado formation. The resulting probability distribution exhibits a systematic increase in tornado probability at higher population density and lower elevation roughness. To obtain a specific quantitative measure of these conditional dependencies, a simple bivariate log-link linear model is fit to the distribution data to yield mean regression coefficients for each quantity. Results indicate that tornado probability, conditioned on population density, decreases by 11% per 10-m increase in elevation roughness over relatively large length scales (15–20 km), and this effect increases by at least a factor of 2 moving toward smaller length scales of 1–5 km. Finally, the elevation roughness effect is found to remain nearly constant with time, whereas the population bias effect decreases with time, consistent with a trend toward improved reporting practices. These results are robust to varying time period and exclusion of EF1 tornadoes.

Our results are consistent with previous research on the topic using county-level or gridded data, including a negative effect of elevation roughness on tornadogenesis at fixed population density (Jagger et al. 2015; Elsner et al. 2016), a decrease in population density bias with time (Elsner et al. 2013), and no time trend in elevation roughness effect (Elsner et al. 2016). Our results for large $L_{ER}$ yield a smaller elevation roughness effect and larger population bias than these prior studies, each by roughly a factor of 2. The reasons for this difference are unclear, though it may be associated with real differences in visibility and surface vegetation between Arkansas and the Great Plains as well as with differences in statistical correlations of elevation roughness and population density between the regions that might plausibly yield an empirical trade-off between the two effects. Importantly, though, our novel method identifies an enhancement in the elevation roughness effect at smaller elevation roughness length

scale down to 1 km, in line with early research by Gallimore and Lettau (1970). Estimation of this scale-dependent effect in the immediate vicinity of individual tornadogenesis points is unique to our methodology, as it is not quantifiable from county-level or coarse-grid data.

Our results in conjunction with the aforementioned studies suggest that local surface elevation variability likely has a real physical effect on tornado formation. We emphasize that this variability is small-scale in that it exerts a minimal impact on the large-scale flow (as opposed to, for example, a major mountain range). Moreover, the magnitude of this terrain effect is empirically large enough to have significant effects on tornado activity and perhaps its impacts on society. However, we currently lack a physical understanding of the pathways through which small-scale surface elevation variability affects tornado formation, which may include the vortex scale (e.g., direct vortex breakdown), the storm scale (evolution of convective storm structure and organization), and/or details of the mesoscale thermodynamic environment in which parent storms develop. This work has identified an enhanced elevation roughness effect on tornadogenesis at small length scales that are perhaps comparable to those of the horizontal scale of a tornado, which may suggest a direct effect of elevation variability on the vortex itself; deeper evaluation of this hypothesis is needed.

There are a number of caveats associated with our analysis. First and foremost, while we have attempted to account for key confounding factors (population, EF1, time period) in the historical tornado record and test for robustness, we are nonetheless reliant on this database and all of its known and unknown deficiencies. Indeed, there may exist other biases in the historical dataset, such as proximity to interstate highways (Blair and Lunde 2010), not captured by population density that warrant closer examination. Additionally, details at scales finer than the resolutions of our elevation and population datasets may yet be important but cannot be captured here. Finally, the extent to which our results can be generalized to much higher elevation roughness values is unclear, nor is it obvious that elevation standard deviation is necessarily the most important measure of elevation roughness relevant to tornado formation.

Following from these caveats, there are myriad avenues for future work. First and foremost, with the recent emergence of tornado-scale physical modeling, idealized physical modeling experiments of small-scale surface elevation variability could yield insight into the pathways by which surface variability affects tornadogenesis in the vein of Lewellen (2014). This could include both detailed understanding of these pathways and how such effects vary across different patterns of elevation variability as well as its magnitude, from gentle hills to mountain ranges. Second, this methodology could be applied to other regions of the country to further test the robustness of our results. Third, a comprehensive apples-to-apples comparison across the range of methodologies used in this and prior studies would help explain quantitative differences in elevation roughness effects and population density biases, as well as other nonpopulation biases not yet accounted for in the literature. Fourth, this approach could be viably applied to a radar-based tornadic signature database whose objective event database would be considered more reliable albeit with a much smaller sample size. Fifth, this work has assumed that the effect of terrain elevation variability is isotropic; consideration of the orientation of terrain relative to tornado path may yield additional empirical insight into the tornado–terrain interaction problem. Similarly, the effect of surface roughness associated with land cover (e.g., lakes, forest, farmland) has not been explored. Finally, this Bayesian framework may be readily extended to incorporate meteorological parameters in addition to the nonmeteorological parameters analyzed here. Doing so could yield a more general, population-adjusted Bayesian tornado probability model useful for real-world prediction at any time scale, from climatological to subseasonal to daily.

*Acknowledgments.* This work is funded in part by NOAA Grant NA16OAR4590208 and by NSF Grant AGS-1648681. The authors thank Robin Tanamachi, Ernie Agee, and three anonymous reviewers for feedback that improved this manuscript.

## REFERENCES

Agee, E. M., 2014: A revised tornado definition and changes in tornado taxonomy. *Wea. Forecasting*, **29**, 1256–1258, https://doi.org/10.1175/WAF-D-14-00058.1.

——, and S. Childs, 2014: Adjustments in tornado counts, f-scale intensity, and path width for assessing significant tornado destruction. *J. Appl. Meteor. Climatol.*, **53**, 1494–1505, https://doi.org/10.1175/JAMC-D-13-0235.1.

Allen, J. T., M. K. Tippett, and A. H. Sobel, 2015: Influence of the El Niño/Southern Oscillation on tornado and hail frequency in the United States. *Nat. Geosci.*, **8**, 278–283, https://doi.org/10.1038/ngeo2385.

Blair, S. F., and E. P. Lunde, 2010: Tornadoes impacting interstates: Service and societal considerations. *Electron. J. Severe Storms Meteor.*, **5** (4), http://www.ejssm.org/ojs/index.php/ejssm/article/viewArticle/64/73.

Bodine, D. J., T. Maruyama, R. D. Palmer, C. J. Fulton, H. B. Bluestein, and D. C. Lewellen, 2016: Sensitivity of tornado dynamics to soil debris loading. *J. Atmos. Sci.*, **73**, 2783–2801, https://doi.org/10.1175/JAS-D-15-0188.1.

Bosart, L. F., A. Seimon, K. D. LaPenta, and M. J. Dickinson, 2006: Supercell tornadogenesis over complex terrain: The Great

Barrington, Massachusetts, tornado on 29 may 1995. *Wea. Forecasting*, **21**, 897–922, https://doi.org/10.1175/WAF957.1.

Doswell, C. A., III, 2007: Small sample size and data quality issues illustrated using tornado occurrence data. *Electron. J. Severe Storms Meteor.*, **2** (5), http://www.ejssm.org/ojs/index.php/ejssm/article/viewArticle/26/27.

——, and D. W. Burgess, 1988: On some issues of United States tornado climatology. *Mon. Wea. Rev.*, **116**, 495–501, https://doi.org/10.1175/1520-0493(1988)116<0495:OSIOUS>2.0.CO;2.

Elsner, J. B., L. E. Michaels, K. N. Scheitlin, and I. J. Elsner, 2013: The decreasing population bias in tornado reports across the central plains. *Wea. Climate Soc.*, **5**, 221–232, https://doi.org/10.1175/WCAS-D-12-00040.1.

——, and Coauthors, 2016: The relationship between elevation roughness and tornado activity: A spatial statistical model fit to data from the central Great Plains. *J. Appl. Meteor. Climatol.*, **55**, 849–859, https://doi.org/10.1175/JAMC-D-15-0225.1.

Gallimore, R., and H. Lettau, 1970: Topographic influence on tornado tracks and frequencies in Wisconsin and Arkansas. *Trans. Wis. Acad. Sci. Arts Lett.*, **58**, 101–127.

Grams, J. S., R. L. Thompson, D. V. Snively, J. A. Prentice, G. M. Hodges, and L. J. Reames, 2012: A climatology and comparison of parameters for significant tornado events in the United States. *Wea. Forecasting*, **27**, 106–123, https://doi.org/10.1175/WAF-D-11-00008.1.

Homar, V., M. Gaya, R. Romero, C. Ramis, and S. Alonso, 2003: Tornadoes over complex terrain: An analysis of the 28th august 1999 tornadic event in eastern Spain. *Atmos. Res.*, **67**, 301–317, https://doi.org/10.1016/S0169-8095(03)00064-4.

Jagger, T. H., J. B. Elsner, and H. M. Widen, 2015: A statistical model for regional tornado climate studies. *PLOS ONE*, **10** (8), e0131876, https://doi.org/10.1371/journal.pone.0131876.

Karpman, D., M. A. Ferreira, and C. K. Wikle, 2013: A point process model for tornado report climatology. *Stat*, **2**, 1–8, https://doi.org/10.1002/sta4.14.

Knupp, K. R., and Coauthors, 2014: Meteorological overview of the devastating 27 April 2011 tornado outbreak. *Bull. Amer. Meteor. Soc.*, **95**, 1041–1062, https://doi.org/10.1175/BAMS-D-11-00229.1.

LaPenta, K. D., L. F. Bosart, T. J. Galarneau Jr., and M. J. Dickinson, 2005: A multiscale examination of the 31 May 1998 Mechanicville, New York, tornado. *Wea. Forecasting*, **20**, 494–516, https://doi.org/10.1175/WAF875.1.

Lawson, J. R., J. S. Kain, N. Yussouf, D. C. Dowell, D. M. Wheatley, K. H. Knopfmeier, and T. A. Jones, 2018: Advancing from convection-allowing NWP to Warn-on-Forecast: Evidence of progress. *Wea. Forecasting*, **33**, 599–607, https://doi.org/10.1175/WAF-D-17-0145.1.

Leslie, F. W., 1977: Surface roughness effects on suction vortex formation: A laboratory simulation. *J. Atmos. Sci.*, **34**, 1022–1027, https://doi.org/10.1175/1520-0469(1977)034<1022:SREOSV>2.0.CO;2.

Lewellen, D. C., 2014: Local roughness effects on tornado dynamics. *27th Conf. on Severe Local Storms*, Madison, WI, Amer. Meteor. Soc., 15A.1, https://ams.confex.com/ams/27SLS/webprogram/Manuscript/Paper254357/SLS14_pap_submit.pdf.

——, B. Gong, and W. Lewellen, 2008: Effects of finescale debris on near-surface tornado dynamics. *J. Atmos. Sci.*, **65**, 3247–3262, https://doi.org/10.1175/2008JAS2686.1.

Manabe, S., and T. B. Terpstra, 1974: The effects of mountains on the general circulation of the atmosphere as identified by numerical experiments. *J. Atmos. Sci.*, **31**, 3–42, https://doi.org/10.1175/1520-0469(1974)031<0003:TEOMOT>2.0.CO;2.

Mooney, C. Z., R. D. Duval, and R. Duvall, 1993: *Bootstrapping: A Nonparametric Approach to Statistical Inference.* Sage, 73 pp.

Natarajan, D., 2011: Numerical simulation of tornado-like vortices. Ph.D. thesis, Western University, 144 pp., https://ir.lib.uwo.ca/cgi/viewcontent.cgi?article=1153&context=etd.

Nelder, J. A., and R. J. Baker, 2004: Generalized linear models. *Encyclopedia of Statistical Sciences*, Vol. 4, S. Kotz et al., Eds., https://doi.org/10.1002/0471667196.ess0866.

Prociv, K. A., 2012: Terrain and landcover effects of the southern Appalachian Mountains on the low-level rotational wind fields of supercell thunderstorms. Ph.D. thesis, Virginia Polytechnic Institute and State University, 87 pp., http://hdl.handle.net/10919/32463.

QGIS, 2015: QGIS geographic information system. Open Source Geospatial Foundation Project, https://qgis.org/en/site/.

Schneider, D. G., 2009: The impact of terrain on three cases of tornadogenesis in the Great Tennessee Valley. *Electron. J. Oper. Meteor.*, EJ11, http://nwafiles.nwas.org/ej/pdf/2009-EJ11.pdf.

Thompson, R. L., R. Edwards, and C. M. Mead, 2004: An update to the supercell composite and significant tornado parameters. *22nd Conf. on Severe Local Storms*, Hyannis, MA, Amer. Meteor. Soc., P8.1, https://ams.confex.com/ams/pdfpapers/82100.pdf.

Tippett, M. K., J. T. Allen, V. A. Gensini, and H. E. Brooks, 2015: Climate and hazardous convective weather. *Curr. Climate Change Rep.*, **1**, 60–73, https://doi.org/10.1007/s40641-015-0006-6.

Verbout, S. M., H. E. Brooks, L. M. Leslie, and D. M. Schultz, 2006: Evolution of the U.S. tornado database: 1954–2003. *Wea. Forecasting*, **21**, 86–93, https://doi.org/10.1175/WAF910.1.